Expression profiles in surgically-induced carotid stenosis: a combined transcriptomic and proteomic investigation

A. Forte [a], M. Finicelli [a], P. De Luca [b], C. Quarto [c], F. Onorati [d], P. Santè [c], A. Renzulli [d], U. Galderisi [a], L. Berrino [a], M. De Feo [c], F. Rossi [a], M. Cotrufo [c], A. Cascino [a, *], M. Cipollaro [a]

[a] Excellence Research Center for Cardiovascular Diseases, Department of Experimental Medicine, Second University of Naples, Italy
[b] BIOGEM S.c.a.r.l., Ariano Irpino, Italy
[c] Excellence Research Center for Cardiovascular Diseases, Department of Cardiothoracic Sciences, Second University of Naples, Italy
[d] Unit of Cardiac Surgery, University Magna Graecia, Catanzaro, Italy

Abstract

Vascular injury aimed at stenosis removal induces local reactions often leading to restenosis. The aim of this study was a concerted transcriptomic-proteomics analysis of molecular variations in a model of rat carotid arteriotomy, to dissect the molecular pathways triggered by vascular surgical injury and to identify new potential anti-restenosis targets. RNA and proteins extracted from inbred Wistar Kyoro (WKY) rat carotids harvested 4 hrs, 48 hrs and 7 days after arteriotomy were analysed by Affymetrix rat microarrays and by bidimensional electrophoresis followed by liquid chromatography and tandem mass spectrometry, using as reference the RNA and the proteins extracted from uninjured rat carotids. Results were classified according to their biological function, and the most significant Kyoro Encyclopedia of Genes and Genomes (KEGG) pathways were identified. A total of 1163 mRNAs were differentially regulated in arteriotomy-injured carotids 4 hrs, 48 hrs and 7 days after injury ($P < 0.0001$, fold-change ≥ 2), while 48 spots exhibited significant changes after carotid arteriotomy ($P < 0.05$, fold-change ≥ 2). Among them, 16 spots were successfully identified and resulted to correspond to a set of 19 proteins. mRNAs were mainly involved in signal transduction, oxidative stress/inflammation and remodelling, including many new potential targets for limitation of surgically induced (re)stenosis (*e.g.* Arginase I, Kruppel like factors). Proteome analysis confirmed and extended the microarray data, revealing time-dependent post-translational modifications of Hsp27, haptoglobin and contrapsin-like protease inhibitor 6, and the differential expression of proteins mainly involved in contractility. Transcriptomic and proteomic methods revealed functional categories with different preferences, related to the experimental sensitivity and to mechanisms of regulation. The comparative analysis revealed correlation between transcriptional and translational expression for 47% of identified proteins. Exceptions from this correlation confirm the complementarities of these approaches.

Keywords: remodelling • cardiovascular surgery • gene array analysis • proteomics

Introduction

Restenosis following vascular injury remains a pressing clinical problem, despite continuous improvements in analysis of predictive markers and trials of new therapeutic strategies. In particular, the introduction of drug-eluting stents (DES) was initially welcome as the solution for long-term restenosis [1] and relegated all other therapeutic approaches to the background. However, it is gradually emerging that rates of late restenosis and thrombosis after the use of DES are higher than suggested by initial experience [2].

Furthermore, angioplasty cannot be always considered the best procedure, depending on the number and localisation of arterial lesions and on comorbidities. In this concern, it has been

*Correspondence to: Amalia FORTE,
Department of Experimental Medicine,
Second University of Naples,
Via L. De Crecchio, 7 - 80138 Naples, Italy.
Tel.: +39-081-5665930
Fax: +39-081-5667547
E-mail: amalia.forte@unina2.it

demonstrated the superiority of bypass over angioplasty in diabetic patients requiring multi-vessel re-vascularization [3].

Carotid artery can be submitted to endarterectomy or to angioplasty to normalize impaired cerebral haemodynamics. Randomized trials did not reveal so far a substantial advantage of the more recently introduced carotid stenting with respect to endarterectomy, that remains a primary choice for treatment of severe symptomatic carotid stenosis [4].

In this context, experimental carotid surgical injury remains a major tool, to dissect the molecular pathways involved in stenosis progression and to identify novel potential targets for (re)stenosis limitation. We set up and validated an arteriotomy model of surgical injury of rat common carotid [5] that has also been used to verify the effectiveness of locally applied antirestenosis drugs [6]. This model mimics the injury affecting the arteries submitted to grafting or endarterectomy, since it is characterized by an interruption of the internal and external elastic lamina, which is considered clinically relevant for the development of arterial stenosis. Our model of arteriotomy, as well as the large majority of studies conducted in animal models of vascular injury, has been applied on healthy, non-stenotic vessels. The exacerbate reparative mechanisms occurring after vascular injury in healthy or atherosclerotic vessels have a common basis, even if with possible differences related to basal increased inflammation, endothelial dysfunction and proliferative activity. Transcriptome and proteome feed back to each other in a highly complex way. To begin to understand the regulatory interactions between transcriptome and proteome, a comparative approach including the simultaneous analysis of expression at the RNA and protein level is required. So far, comparative and transcriptome and proteome analyses have been conducted mainly on cultured prokaryotic and eukaryotic cells, while data obtained in complex organisms are very limited [7]. This is the first study combining a transcriptomic and proteomic analysis of differential gene expression in a model of (re)stenosis, and more precisely during the acute phase that follows carotid arteriotomy, using high-density microarrays and Real Time RT-PCR for mRNA analysis and bidimensional (2D)-gel electrophoresis followed by liquid chromatography (LC) and tandem mass spectrometry (MS/MS) for protein identification.

Our microarray data included a number of genes that could represent new putative targets for prevention of surgically induced stenosis and showed a partial correlation with proteomics data, confirming the complementarities of both approaches.

Methods

Animals

Studies were carried out on 12-week-old inbred male WKY rats (300–310 g) (Charles Rivers, France). All animals were handled in compliance with the 'Guide for the Care and Use of Laboratory Animals' published by the US National Institute of Health (NIH publication No. 85-23, revised 1996). All protocols were approved by the Animal Care and Use Committee of the Second University of Naples. Rats were acclimatized and quarantined for at least 1 week before undergoing surgery.

Vascular injury

Arteriotomy of rat common carotid artery was performed as already published [6]. Briefly, a plastic Scanlom clamp for coronary artery grafting was placed for 10 sec. on the carotid causing a crushing lesion to the vessel. At the same point where the clamp was applied, a 0.5 mm longitudinal incision was done on the full thickness of the carotid. The incision did not cross to the other side of the vessel. Haemostasis was obtained with a single adventitial 8.0-gauge polypropylene stitch. Once bleeding stopped, the carotid artery was carefully examined and blood pulsation was checked distally to the incision.

Histological analysis

Carotid arteries were harvested 4 hrs, 48 hrs, 7 days, 14 days, 21 days and 30 days after arteriotomy (n = 4 for each group). The vessels were fixed in 4% buffered formaldehyde, dehydrated and embedded in paraffin. 5 μm cross-sections were stained with haematoxylin-orcein for nucleus and elastic fibre staining, respectively. Image screening and photography of serial cross-sections were performed using a Leica IM 1000 System. Lumen and medial areas were measured using the Leica IM 1000 software. The lumen and medial areas of each injured carotid were normalized with respect to the ipsilateral distal region. Measurements were performed by two independent observers.

RNA extraction/labelling

Carotid segments were harvested 4 hrs, 48 hrs and 7 days after arteriotomy (n = 3 pools of five carotids each for all groups). Total RNA was extracted from injured carotids and from pools of carotids from uninjured rats (n = 15) using the RNeasy mini kit (Qiagen). During extraction, RNA was treated with DNase (Qiagen) to remove DNA contamination. RNA concentration was measured using a NanoDrop ND-1000 spectrophotometer (NanoDrop Technologies). Total RNA integrity was verified by electrophoresis on denaturing 1% agarose gel containing highly sensitive 2x GelStar Nucleic Acid Stain (Lonza) to ensure the absence of sample degradation. Absence of residual DNA was verified by PCR on total RNA without reverse transcription. 200 ng of each RNA sample were amplified and biotin-labelled with two rounds of amplification following the Affymetrix small sample labelling protocol.

Microarray hybridization and analysis

15 μg of each biotinylated cRNA were hybridized to Genechips 230 2.0 (Affymetrix), containing over 31,000 genes and open reading frames from *R. norvegicus* Genome databases GenBank, dbEST and RefSeq. Three replicates for each point were hybridized. The microarrays were then washed and scanned according to manufacturer's protocols (www.affymetrix.com/support/technical/manual/expression manual.affx) on the Affymetrix Complete GeneChip® Instrument System. Digitized

image data (DAT) files were analysed by MAS 5.0 (Affymetrix Inc, Santa Clara, CA, USA). for detection calls. The expression values obtained were analysed by GeneSpring 7.3 (Silicon Genetics, Santa Clara, CA, USA). Results were filtered for flag (presence call), then for fold-change (FC) ≥ 2, obtaining a total of 15,600 probe sets differentially expressed in the different conditions.

Statistical analysis was performed by the two-way ANOVA using a parametric test with variances assumed equal, P-value cut-off 0.0001. The Bonferroni multiple testing correction was applied. The false discovery rate in these conditions was proximal to zero (Supplemental file 1). Final data comply with the minimum information about a microarray experiment (MIAME) requirements and have been loaded in the European Bioinformatics Institute (EBI) database with the accession number E-MEXP-1278 (www.ebi.ac.uk). Differentially expressed genes were grouped for similar biological processes according to gene ontology (GO) definitions (www.geneontology.org) (supplemental file 2). A gene was associated with a GO term if it was annotated by this term or by its child. Hierarchical clustering was performed on the gene lists by the gene tree algorithm using as similarity measure the Pearson correlation and the clustering algorithm average linkage.

Significant biological pathways implicated in time-dependent carotid reaction to arteriotomy and gene product association networks have been identified through DAVID (Database for Annotation, Visualization and Integrated Discovery) at http://david.abcc.ncifcrf.gov and by BioRag (Bioresource for array genes) at http://www.biorag.org (Supplemental file 6).

Quantitative real-time RT-PCR

Quantitative real-time PCR (MJ Opticon II, Bio-Rad) was used to determine the copy number of mRNA for nine genes (c-myc, Vegf, Trpc6, vWF, Fn ED-A, Id2, Map2, Gfap, Agt) in arteriotomy-injured carotids in comparison to carotids from uninjured rats. Validation of the microarray data was considered to be a significant ($P < 0.05$) change in normalized PCR copy number in the same direction found in the microarray data. cDNA was generated from 400 ng of each RNA sample used for microarray hybridizations. Reverse transcription was done at 42°C for 1 hr in presence of random examers and Moloney-Murine Leukemia Virus (M-MULV) reverse transcriptase (Finnzymes). PCR primer pairs, designed by the Primer express software (Applied Biosystems, Foster City, CA, USA), were chosen to yield 100–150 bp products and were validated running the PCR products on agarose gel to confirm a single band. In addition, melting curves from 65°C to 94°C were generated to determine whether there were any spurious amplification products. GAPDH was chosen as reference house keeping gene. Relative quantitative RT-PCR was used to determine the fold difference for genes. The PCR efficiency was determined for each primer pair and was calculated using a dilution series and MJ Opticon II analysis software.

Protein extraction

Rat carotid segments were harvested 4 hrs, 48 hrs and 7 days after arteriotomy (n = 5 for each group) and from uninjured rats (n = 5). Carotids were rinsed thoroughly with cold phosphate-buffered saline to remove blood components and frozen immediately in liquid nitrogen. The frozen tissue was disrupted and lysed in a buffer containing 9.5 M Urea, 2% CHAPS, 0.8% Pharmalyte pH 4–7, 1% Dithiothreitol (DTT) and protease inhibitor cocktail. Protein concentration in the supernatants was assessed using a modified version of Bradford assay.

2-DE

100 μg of each sample for analytical 2D-gels were diluted into rehydration buffer (8 M Urea, 0.5% CHAPS, 0.2% DTT, 0.2% Pharmalyte pH 4–7) for the overnight re-swelling of immobilized pH gradient (IPG) strips (4–7 L; 18 cm, Amersham Biosciences, Piscataway, NJ, USA) prior to isoelectric focusing, carried out at 0.05 mA/IPG strip; 5 W power max; 3500–75,000 V h; 20°C followed by electrophoretic separation on 12% polyacrylamide gels. Analytical gels were stained with OWL silver staining kit (Insight Biotechnology Ltd., Wembley, UK) and scanned at 100-μm resolution using a molecular dynamics personal SI laser densitometer (Sunnyvale). Protein spots were analysed quantitatively using the PDQuest 2-D software (Bio-Rad). Protein abundance was quantified by measuring the normalized optical density (taken as a fraction of the total optical density of valid spots on the gel) of each protein spot. Differentially expressed spots were identified (FC ≥ 2), statistical analysis was performed by the two-way ANOVA (P-value cut-off 0.05) and a spot pick list was generated.

Preparative gels were loaded with 400 μg of each sample and stained with the PlusOne silver staining kit (Amersham Biosciences, Piscataway, NJ, USA) with slight modifications to ensure compatibility with subsequent MS analysis. Preparative gel images were incorporated into a set of analytical gel images and matched. Images were calibrated for Molecular Weight (MW) and pI and spots were excised.

Enzymatic Digestion, LC/MS/MS and Database Searching

In-gel reduction, alkylation and digestion with trypsin were performed prior to subsequent analysis by MS. Cysteine residues were reduced with dithiothreitol and derivatised by treatment with iodoacetamide to form stable carbamidomethyl derivatives. Trypsin digestion was carried out overnight at room temperature after an initial 2 hr incubation at 37°C. Peptides were extracted from the gel by a series of acetonitrile and aqueous washes. The extract was pooled with the initial supernatant and lyophilized. Each sample was then re-suspended in 50 mM ammonium bicarbonate and analysed by LC/MS/MS. Chromatographic separations were performed using an Ultimate LC system (Dionex, UK). Peptides were resolved by reversed phase chromatography on a 75 μm C18 PepMap column. A gradient of acetonitrile in 0.05% formic acid was delivered to elute the peptides at a flow rate of 200 nl/min. Peptides were ionized by electrospray ionisation using a Z-spray source fitted to a QTof-micro (Waters Corp., Melford, MA, USA) The instrument was set to run in automated switching mode, selecting precursor ions based on their intensity, for sequencing by collision-induced fragmentation. The MS/MS analyses were conducted using collision energy profiles that were chosen based on the m/z and the charge state of the peptide. The mass spectral data was processed into peak lists and searched against the Swiss Prot or National Center for Biotechnology Information non-redundant databases using Mascot software (Matrix Science, UK). The data was searched using specific amino acid modification parameters, that is variable cysteine carbamidomethylation modification (resulting from reduction and alkylation reaction) and variable methionine oxidation modification.

Statistical analysis

All statistical analysis was performed using GraphPad software (Prism 4.0). Statistical significance was determined using two-way analysis of variance (ANOVA) followed by Bonferroni's multiple comparison test.

Results

Histological analysis of arteriotomy-induced negative remodelling

Morphological analysis of cross-sections of carotids harvested from 4 hrs up to 30 days after arteriotomy showed changes mainly related to negative remodelling, while the role of intima hyperplasia proved quite limited. In Figure 1, we reported microphotographs of carotids harvested with the same timing used for transcriptome and proteome analysis, with the exception of carotids harvested 4 hrs after arteriotomy, since at this stage reparative and proliferative phenomena were not yet evident at morphological level.

In the adventitia, a pooling of extracellular matrix (ECM) and granulation tissue were observed close to the polypropylene stitch, causing a lumen reduction for compression *ab-estrinseco* of the artery. We also observed an increase of adventitial *vasa vasorum*, presumably related to hypoxia induced by carotid clamping before arteriotomy. The presence of foreign body giant cells was probably related to the polypropylene stitch. A gradual proliferation of Smooth Muscle Cells (SMC) and accumulation of new elastin laminae concomitant with disruption and fragmentation of pre-existing fibres was also observed in the injured media and adventitia (Fig. 1). SMCs and their switching from fully differentiated to proliferating synthetic phenotype were identified in arteriotomy-injured carotids by confocal immunohistochemistry for SM22, an early marker of differentiated SMCs (data not shown). Morphometric analysis revealed a progressive lumen reduction, with a maximal $60 \pm 9\%$ narrowing 30 days after arteriotomy ($P<0.05$).

Microarray transcriptome analysis in arteriotomy-injured carotids

Statistical analysis of microarray data showed consistency in gene expression amongst the replicates within each experimental group, but evidence of substantial transcriptional differences at different times after arteriotomy. This allowed the application of stringent statistical analysis without losing useful information. A total of 1163 mRNA were significantly affected at any time after arteriotomy and are given in Supplemental file 1. Gene names, gene descriptions, biological function, Affymetrix Ids, accession numbers and expression levels are provided.

In more detail, 980, 709 and 612 mRNAs were altered ranging from 4 hrs to 7 days after arteriotomy. Among them, the biological characteristics of 620 genes that were differentially expressed at least in one time-point after arteriotomy were definite and their functions were examined. Heat map in Figure 2 highlights, through a reference colour scale (green = 0; red = 5), the different temporal trends exhibited by functional categories. For example, genes included in cytoskeleton and contractile apparatus and in neurophysiological process GO categories clearly showed a biphasic up-regulation 4 hrs and 7 days after arteriotomy, while other groups of genes (*e.g.* nucleic acid metabolism and protein metabolism) exhibited a marked up-regulation only 4 hrs after arteriotomy and then gradually decreased to basal levels. Figure 3 highlights the number of modulated genes for each functional GO category at different times after arteriotomy. Genes included in each functional GO category are listed and described in supplemental file 2. The remaining 543 transcripts were expressed sequence tags (ESTs) and were also listed in supplemental file 2 and clustered according to their expression profile in supplemental file 3.

Microarray data have been further analysed to identify significant functional pathways involved in arteriotomy-induced stenosis. A total of 16 most significant KEGG pathways ($P<0.1$) have been identified by conjunct application of DAVID and BioRag software (Table 1). Supplemental file 6 provides the full list of genes included in each most significant pathway and in other pathways with a $P>0.1$. The gene product association networks extracted from these 16 KEGG are shown in Figure 4A and B. The core of the network in Figure 4A is constituted by genes involved in MAPK signalling (green line), cell adhesion (yellow line) and focal adhesion (red line).

Among the results we obtained, inflammation-related genes were over-represented, in particular 4 hrs and 48 hrs after arteriotomy, when about 70 genes resulted to be activated. Also the magnitude of their FC was greater 4hrs after injury. Among interleukines (IL), we detected a maximal 135-fold increase of mRNA coding for IL-6, together with an increase of IL-1α and of IL-1β. Among the chemokines, we observed a marked increase of monocyte chemoattractant protein-1 (Mcp-1 or Ccl-2) and of Cxcl2 (or Mip-2).

Moreover, we would like to mention an increase also of Arginase I, included in proline and arginine metabolism KEGG pathway (Fig. 4B and Table 1), and known to be involved in regulation of vascular tone and inflammation.

Inflammation can be stimulated by oxidative stress: in this concern, microarray data highlighted an up-regulation of NAD(P)H oxidase subunits (22phox, gp91phox and Ncf4), of the small GTPase Rac2 and of the antioxidant Sod2, involved in the metabolism of reactive oxygen species (ROS).

In the context of vascular remodelling, we detected an increase of α- and γ-tropomyosin, α-actin 1, myosin heavy and light chains and troponin isoforms, particularly evident 7 days after arteriotomy.

Catecholamines are endowed with vasoconstrictive and growth factor-like activity: we detected a maximal 100-fold increase of dopamine β hydroxylase (Dbh) 7 days after arteriotomy, but no significant change of adrenergic receptor subtypes. Conversely, we observed an increase of cholinergic receptors Chrna7 and Chrnd.

Microarray data indicated an up-regulation of myofibroblast markers, and in particular of fibronectin (Fn) splice variant ED-A, transforming growth factor-β_1 (TGF-β1) receptor II, tenascin C and α-actin.
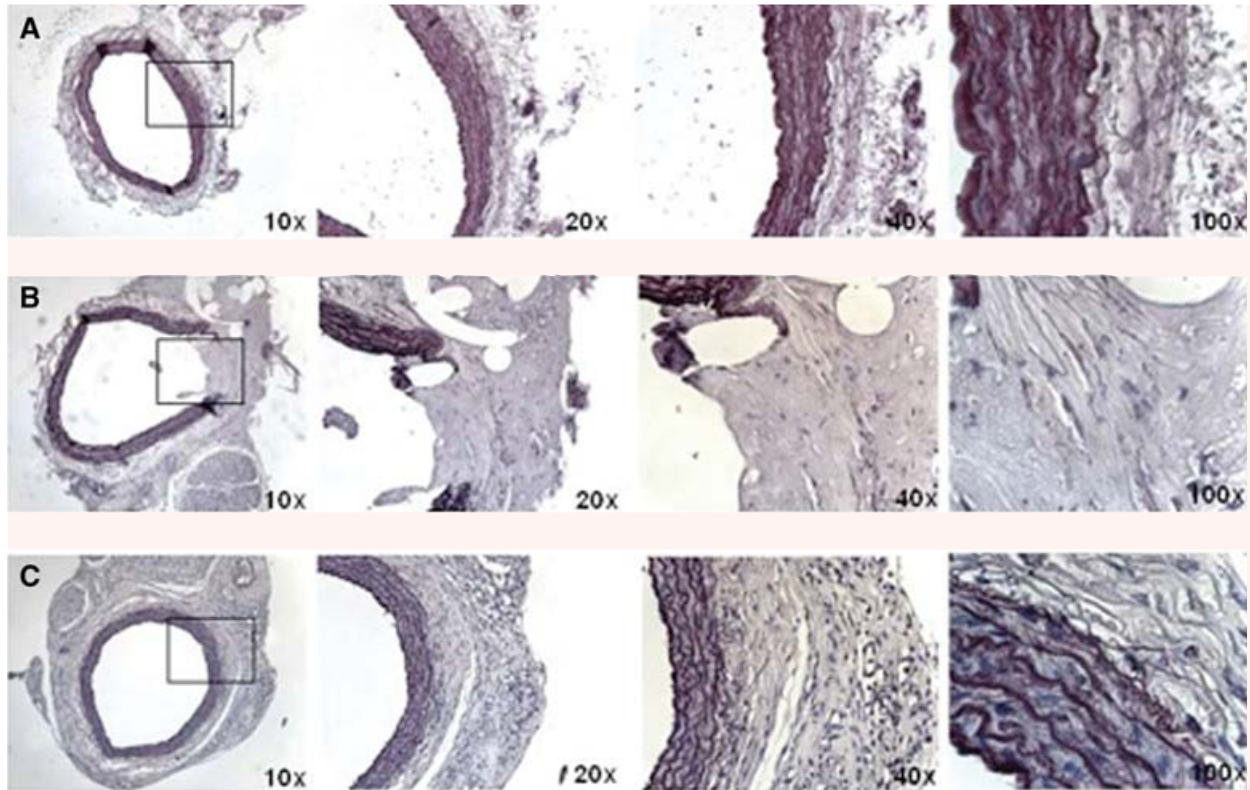
Fig. 1 Representative cross-sections of rat carotids (hematoxylin-orcein staining, 10×, 40× and 100× magnification). Uninjured carotid (**A**) and injured carotid harvested (**B**) 48 hrs and (**C**) 7 days after arteriotomy.

Among the several transcription factors identified by microarray analysis, we would like to mention the Krüppel-like factors (KLFs), known to be involved in many vascular functions. In particular, we observed an increase of KLF4, KLF5, KLF6 and KLF10 since 4 hrs after arteriotomy. Conversely, the KLF15 acting mainly as a repressor of transcription, resulted to be markedly and persistently decreased after arteriotomy.

Finally, we would like to mention the up-regulation of mRNAs involved in stem cell homing at the injury site. Among them, we detected a maximal 4.73-fold increase of the chemokine Cxcl12 (or Stromal cell-derived factor 1 (SDF-1α)), released in the plasma by SMCs and able to mediate the mobilization of bone marrow-derived SMC progenitor cells (SPCs) through the corresponding receptor CXCR4, also increased, but to a lesser significant level ($P < 0.001$). Finally, we detected an increase of Mcp-1, known to recruit endothelial progenitor cells (EPCs) at the injury site.

All the above mentioned results and the overall expression profiles listed in supplemental file 1 clearly reflect the involvement of all the different cell populations present in the injured carotid wall (SMCs, endothelial cells, fibroblasts, inflammatory cells and, possibly, stem cells recruited at the injury site).

Real Time RT-PCR validation of microarray data

Real Time RT-PCR was done on a subset of transcripts either up- (c-myc, Vegf, Fn, Trpc6, Map2, Gfap, Agt) and down-regulated (vWF, Id2, Agt) after arteriotomy. The transcripts were chosen as representative of different functional categories and of biological interest to arterial stenosis, displaying a FC ranging from a high magnitude to near the 2-fold cutoff.

The trend of Real Time RT-PCR results overlapped with microarray data, although the magnitude of the FC resulted to be different (Table 2). For three genes (Gfap, Map2 and Trpc6), the Real Time RT-PCR revealed significant changes also 48 hrs after arteriotomy, that were not showed by microarrays. This could be related to the greater sensitivity of the Real Time PCR compared to the microarray technique, or to standard deviation in microarray replicates, that lead to filtering out some results during statistical analysis.

Since the Fn probe set on microarrays did not allow the distinction among Fn splice variants, we selected a primer pair specific for the rat Fn ED-A variant, a marker of differentiated myofibroblasts, that revealed a maximal 6.7-fold increase 7 days after arteriotomy.
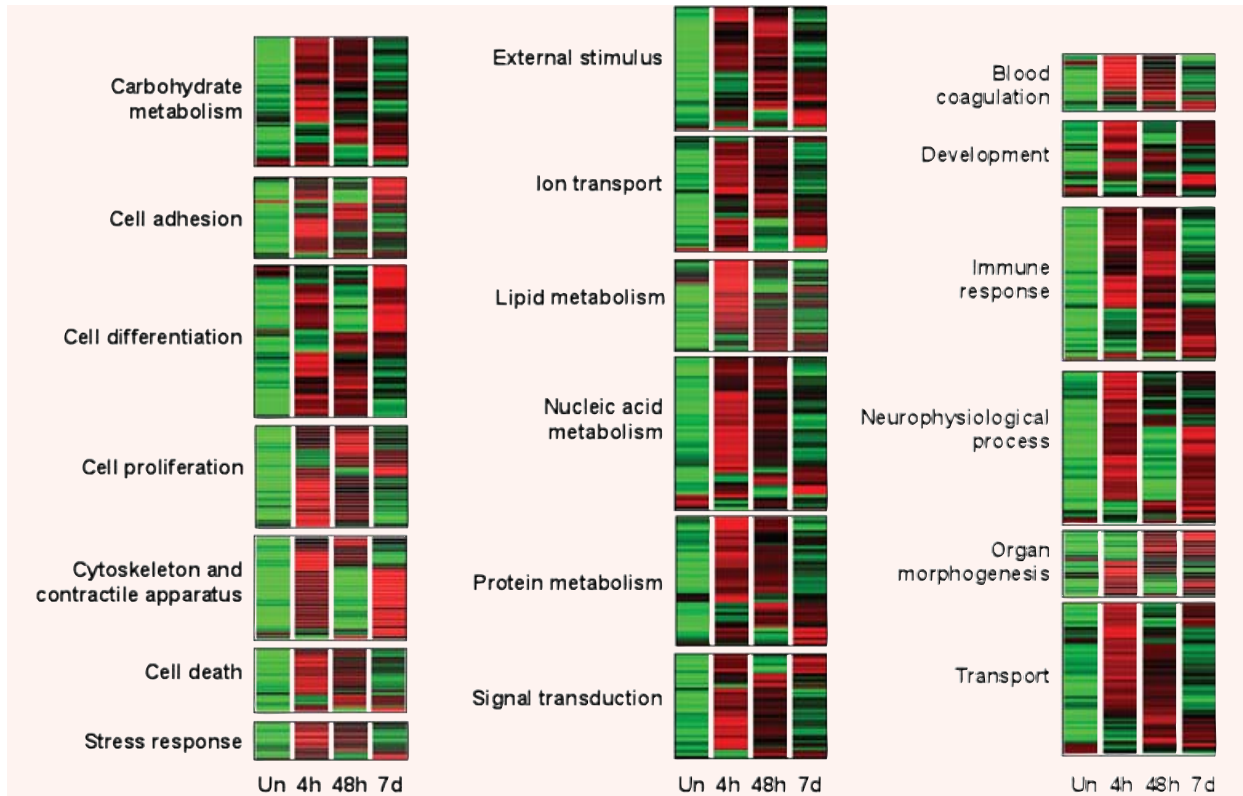
Fig. 2 Time-dependent expression of genes clustered in functional groups. Each row corresponds to a single gene; each column corresponds to the mean of three different experiments (reference colour scale: green = 0; red = 5).

Bidimensional electrophoresis of proteome in arteriotomy-injured carotids

Proteins were extracted from rat carotids harvested with the same timing used for microarrays and were separated on analytical 2D-gels (Fig. 5). A mean of 2093 protein spots were matched and quantitated in analytical 2D-gels for the four groups of carotid samples (uninjured carotids, 4 hrs, 48 hrs and 7 days after arteriotomy), without significant differences in spot number after carotid arteriotomy. Only spots appearing in all the five analytical gels for each group were further considered for statistical analysis. As for the microarray analysis, we selected protein spots whose intensities changed by 2-fold or greater after carotid arteriotomy. Based on these stringent criteria, only a set of 48 spots (0.02%) exhibited significant quantitative changes in arteriotomy-injured carotids (P<0.05). 21 spots were submitted to LC/MS/MS (Supplemental file 5) while the remaining 27 spots were of very small/faint nature and unable to be excised from preparative gels for identification. We considered as valid only proteins identified by at least two peptides, with a Mascot score ≥50 and with a sequence coverage ≥20%. On this basis, we selected only 16 out of the 21 spots analysed by

LC/MS/MS, that resulted to correspond to a set of 19 proteins (Table 3). Among them, two proteins, tropomyosin β chain and heat shock cognate 71 kD protein were not represented by probe sets in microarrays. Of the remaining 17 proteins that were represented by at least a probe set on the microarrays, eight proteins (47%) exhibited a temporal expression profile in agreement with variations of related mRNAs (Table 4). The remaining nine proteins (53%), even if represented by at least a probe set in microarrays, were not included among differentially expressed mRNAs, implying a regulation at translational or post-translational level.

Three proteins (haptoglobin, Hsp27, and contrapsin-like protease inhibitor 6 precursor) were identified within two or three individual spots included in charge trains, suggesting that these major differential proteins are present in different isoforms or with different post-translational modifications (PTM).

In more detail, haptoglobin was identified in spots 6820, 6958 and 6825 (Fig. 6), constituting a charge train in which spot 6820 represented the more acidic one and was absent in uninjured carotids but activated 48 hrs after arteriotomy (Table 3). Spots 6958 and 6825, already present in uninjured carotids, showed a significant 55- and 21-fold increase 48 hrs after arteriotomy, respectively.
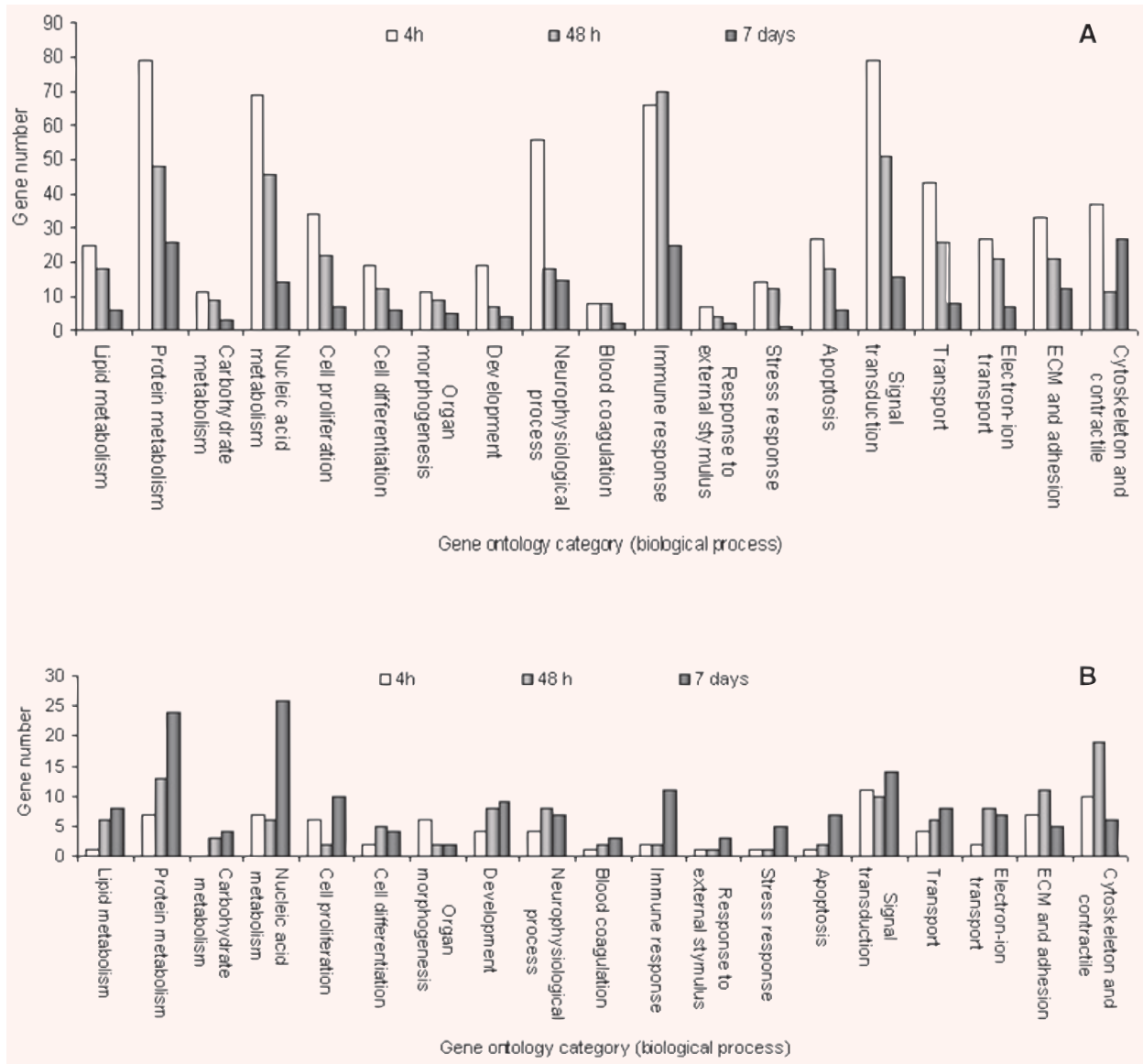
Fig. 3 Functional gene ontology (GO) classification of genes up-regulated (**A**) and down-regulated (**B**) by rat carotid arteriotomy.

Contrapsin-like protease inhibitor 6 precursor (Serpina3n) was identified in spots 6703 and 1036, also part of a charge train, showing a 5.7- and 5.1-fold increase 48 hrs after arteriotomy (Table 3).

Other proteomics results included variations of proteins mainly involved in actin fibre remodelling and in contractility (gelsolin, Hsp27, α and β subunits of F-actin capping protein, α-actin cardiac and smooth muscle isoforms, tropomyosin 2). In particular, Hsp27 showed a pI of 5.38 *vs.* the theoretical 6.12, indicating a 2.82-fold increase of a multi-phosphorylated isoform of this protein 7 days after arteriotomy.

Discussion

Concerted transcriptomic-proteomic strategies in vascular surgery

The combined transcriptomic-proteomic analysis applied to arteriotomy revealed different and complementary potentialities of microarray and protein 2D-elecrophoresis.

High-density microarrays identified a large number of transcripts involved in arteriotomy-induced stenosis, allowing the

Table 1 Most significant KEGG pathways identified by DAVID software in arteriotomy-injured carotids. The number of genes included in each pathway at different points after arteriotomy and the *P*-values are reported. Networks between genes included in pathways are showed in Figure 4.

	Number of genes			Significance		
KEGG pathways	**Time after arteriotomy**			**Time after arteriotomy**		
Cellular and regulatory pathways	**4 hrs**	**48 hrs**	**7 days**	**4 hrs**	**48 hrs**	**7 days**
Focal adhesion	30	20	16	1.7E-5	4.9E-3	2.8E-2
ECM-receptor interaction	12	11	9	6.5E-3	3.4E-3	1.4E-2
Antigen processing and presentation	12	13	13	2.8E-2	1.6E-3	4.7E-4
Cell adhesion molecules (CAMS)	19	15	17	9.9E-3	2.4E-2	1.1E-3
Haematopoietic cell lineage		11			3.8E-3	
Leukocyte transendothelial migration	15	13		1.6E-2	1.3E-2	
B cell receptor signalling pathway	10			2.8E-2		
Cytokine-cytokine receptor interaction	17	15	12	2.6E-2	1.6E-2	6.0E-2
Toll-like receptors signaling pathway	10	10		3.7E-2	8.9E-3	
MAPK signalling pathway	26			6.1E-3		
Complement and coagulation cascades	8		7	6.5E-2		3.5E-2
Cell communication			10			5.1E-2
Type I diabetes mellitus		9	9		2.4E-2	1.1E-2
Apoptosis	10			7.5E-2		
Tgf-β signalling pathway	9	8		6.8E-2	5.4E-2	
Metabolic pathways						
Arginine and proline metabolism	6			9.7E-2		

dissection of patterns that could have not been discovered through analysis of individual genes. Microarrays were used in association with a method developed for mRNA linear amplification [8], that allows the analysis of low amounts of RNA without affecting the fidelity of detection of differential gene expression and the false positive rate [9]. Sample pooling before RNA extraction was necessary because of the low yield of RNA obtained from single samples, as we extracted RNA only from the small carotid segments submitted to arteriotomy (less then 2 mm in length). Carotid pooling allowed the recovery of a sufficient amount of RNA for check of sample integrity, check of absence of DNA, microarray hybridization and quantitative Real Time RT-PCR for data validation.

We used a large base of biological samples (n=15 rats for each point) and stringent parameters to filter the data to avoid false gene identification and assign a level of significance to the overall results. Moreover, a rigorous evaluation of the adequacy of the control condition lead us to use as reference the RNA from carotids harvested from uninjured rats and not from contralateral uninjured carotids, as these latter also showed variations of gene expression, related to a systemic inflammatory reaction and to compensatory reactions that were distinct from those occurring in arteriotomy-injured carotids (manuscript in preparation). On this basis, all time points were compared with a common denominator represented by carotids from uninjured rats, and consequently time courses have been able to be directly compared with each other. A similar strategy has been followed in other microarray-based studies of restenosis [10, 11].

Microarray technology has already been applied in angioplasty-injured carotids [10, 11]. Our work complements these studies as we focused the analysis on early events that trigger long-term negative remodelling in a surgical injury model distinct from angioplasty. A direct comparison of data obtained in arteriotomy- and in angioplasty-injured rat carotids [10] 7 days after procedure (a point common to both protocols) highlighted that only a limited number of mRNAs (n = 152) was affected in both models of injury (Supplemental file 4), thus confirming the differences between these models of vascular injury and suggesting the necessity for different approaches to control arterial restenosis. The reliability of this comparison was sustained by the use of the same microarray technology (Affymetrix). Nevertheless, differences between the two studies, summarized in Figure 6, should be carefully considered. Interestingly, some genes showed an opposite expression profile in the two injury models, with possible divergent consequences on vascular pathophysiology. In particular, Thioredoxin-interacting protein, a thioredoxin natural inhibitor, was increased
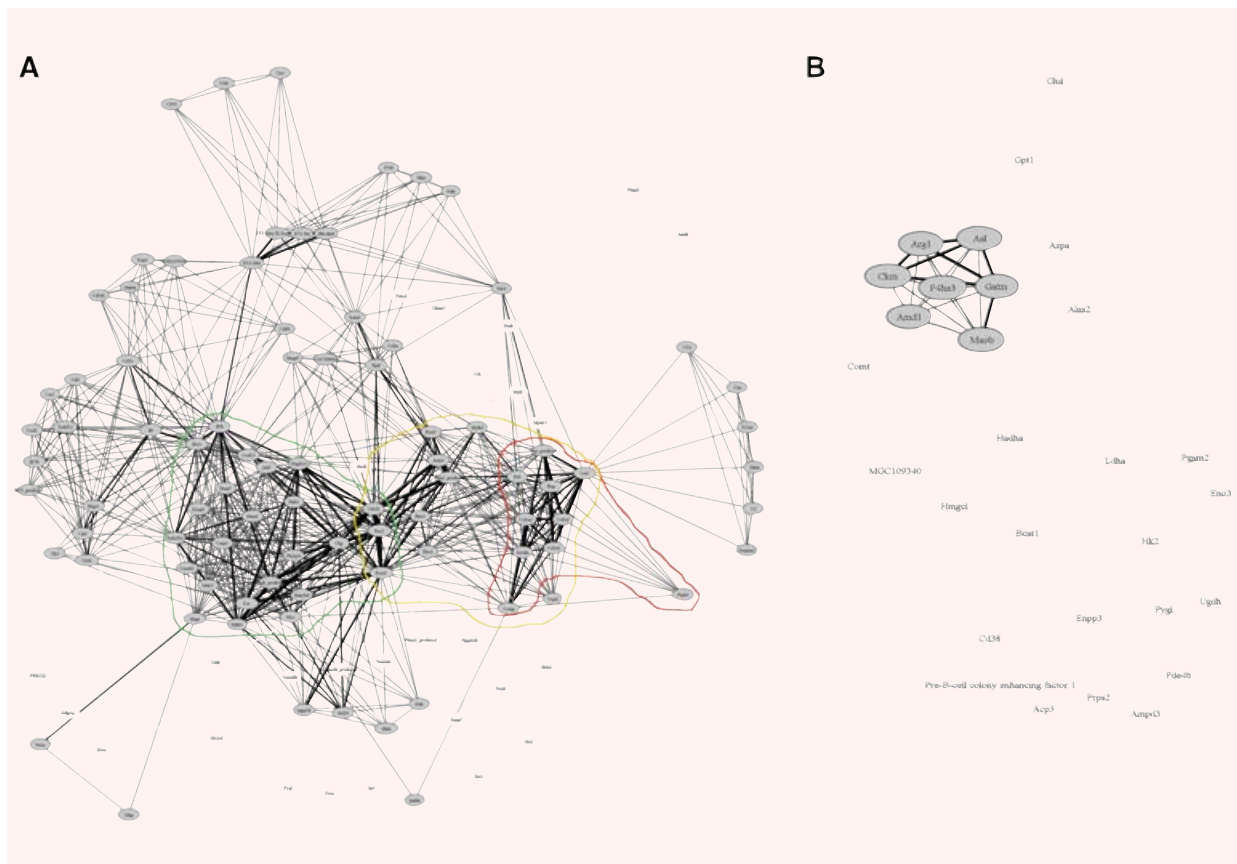
Fig. 4 Gene product association networks extracted from the most significant (**A**) cellular and regulatory process pathways and (**B**) metabolic pathways involved in arteriotomy-induced carotid stenosis (listed in Table 1). The core of the network in A is constituted by genes involved in MAPK signalling (green line), cell adhesion (red line) and focal adhesion (yellow line). The most significant pathway in B is arginine and proline metabolism. Faded nodes belong to pathways with a *P* > 0.1. The thickness of the edge is proportional to the number of pathways to which are associated two genes.

after arteriotomy, while it was permanently down-regulated after angioplasty. This observation, together with the absence of other genes involved in ROS production in angioplasty-injured carotids [10], further supports a sustained oxidative stress induced by arteriotomy.

Proteomic analysis resulted in a more limited amount of information in comparison to microarrays (19 identified proteins *versus* 1163 mRNA differentially expressed in arteriotomy-injured carotids), but it was at level of protein synthesis and provided data also about PTM, that determine to a large extent the function and fate of the protein. Indeed, improper protein modifications might alter the function of the cells, and might be characteristic of the disease.

Proteome analysis is still affected by experimental limits, represented by the difficulty in detecting and analyzing very low-abundance proteins (*e.g.* regulatory proteins), as well as hydrofobic, insoluble,

very basic, very small and very large proteins [12]. It has been estimated that the detection limit of the proteomic approach is to at least 1000 copies of a protein per cell [7].

Proteomic datasets of SMCs [13, 14] and endothelial cells (ECs) [15] represent a useful reference for proteomics in vascular research, but the proteome analysis after tissue injury is still limited [12].

The information we obtained with standard proteomics techniques was probably limited also by the characteristics of vascular tissue, in which 90% of proteins is represented by members of the cytoskeleton and contractile apparatus, above all actins, thus making difficult the identification of low-abundant proteins. Because of the very different size of proteome and transcriptome databases obtained from arteriotomy-injured carotids, we did not conduct a global scale correlation analysis of protein and mRNA levels.

Table 2 Relative changes of gene expression as assessed by Real Time RT-PCR in injured carotids harvested 4 hrs, 48 hrs and 7 days after arteriotomy and comparison with related microarray data (n = 3 RNA pools for each point). Only statistically significant variations (*P*<0.05) of gene expression in comparison to uninjured carotids were reported.

| Gene name | Affymetrix Probe Set ID | Fold-change of signal | | | | | |
| | | Real Time RT-PCR | | | Microarray | | |
		4 hrs/ Uninjured carotids	48 hrs/ Uninjured carotids	7 days/ Uninjured carotids	4 hrs/ Uninjured carotids	48 hrs/ Uninjured carotids	7 days/ Uninjured carotids
c-myc	1368308_at	11	2.4		20.98	3.744	
Vegf	1373807_at	2.24			2.64		
ED-A Fn	1370234_at		6.55	6.7		2.66	2.383
TRPC6	1370139_at	2.94	0.23	0.74	12.19		2.941
vWF	1389234_at	0.71	0.12	0.2	0,307	0.228	0.312
Id2	1368870_at	0.21	0.17	0.13	0.132	0.273	0.395
Map2	1388152_at	1.04	2.9	1.2	2.147		2,57
Gfap	1368353_at	36.7	56.3	54.4	49.56		4.46
Agt	1387811_at	1.17		0.82	2.125		0.369

The comparison of the functional annotation of the differential proteins and mRNAs identified in arteriotomy-injured carotids suggests that proteomics and microarray detection methods reveal functional categories with different preference (Fig. 7). In more detail, differential microarray analysis of arteriotomy-injured carotids revealed a large number of diverse functions, and signal transduction, nucleic acid metabolism and inflammation GO functional categories include the largest fraction of known mRNAs identified. In contrast, differential proteome analysis revealed a lower number of different functional GO categories, with the cytoskeleton and contractile apparatus, protein metabolism and stress response constituting the largest fraction of identified proteins. This difference is probably related to the experimental limitation of the proteomic techniques and to the higher sensitivity of microarray analysis. Improved proteomic techniques (*e.g.* Differential In Gel Electrophoresis) will certainly increase resolution and sensitivity, providing adjunctive information at proteome level in the analysis of vascular pathophysiology.

Microarray transcriptome analysis in arteriotomy-injured carotids

Among the 1163 genes identified by microarray analysis, there are several new potential targets for therapy. We would like to focus the discussion of microarray data mainly on genes involved in inflammation/oxidative stress, ECM metabolism and wound healing, as these processes appear of particular interest in arteriotomy. Inflammation plays a striking role in response to vascular injury and in general in the risk of cardiovascular disease. Humoral factors released by vascular cells and by perivascular tissues immediately after the injury play mainly an autocrine or paracrine function, while others are released in the serum and can exert a systemic effect on distant uninjured sites. Different humoral factors are released in plasma after carotid injury [16]. The liver is the major source of circulating plasma proteins during inflammation and can be the target itself of mediators secreted peripherally at the injury site. IL-6 and IL-1, both increased 4 hrs after arteriotomy and known to be secreted by activated monocytes and SMCs, can exert paracrine effects on cell proliferation and play a major role as mediators of the hepatic acute-phase reaction, by activating the JAK/STAT pathway in the hepatocytes, which in turn accounts for the induction of circulating biomarkers of vascular inflammation with a significant cardiovascular action [17].

Mcp-1 is another soluble pro-inflammatory mediator increased in arteriotomy-injured carotids. Our data are in agreement with studies revealing its rapid increase in the arterial wall and in the circulation after injury [18]. Mcp-1 exerts its effect, at least in part, by inducing ROS generation, which in turn can further enhance the synthesis of Mcp-1 through an autocrine mechanism, and/or evoke a secondary cytokine and growth factor response (Vegf, Igf, Fgf, all induced by arteriotomy) in the injured vascular wall.

Arginase I, classically considered exclusive to the liver, has been found also in other tissues, including the vessels [19]. This enzyme, member of a nitric oxide-synthase (NOS)-alternative pathway for L-Arginine breakdown leading to biosynthesis of urea and L-ornithine, plays a role in the regulation of vascular tone and is involved in vascular dysfunctions (*e.g.* hypertension). To our knowledge, our data highlight for the first time the increase of Arginase I in vascular injury.
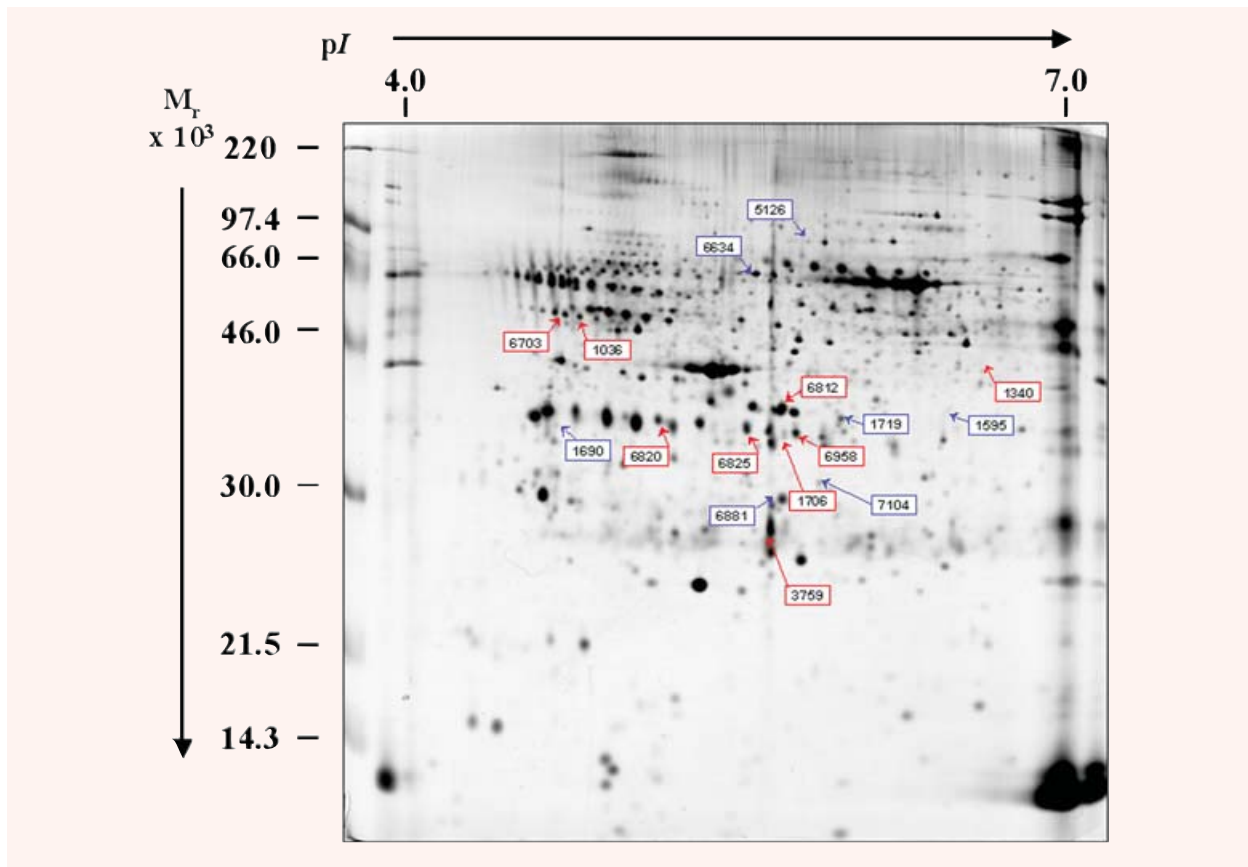
Fig. 5 Reference analytical 2D-gel of proteins from a rat carotid harvested 48 hrs after arteriotomy. 1st dimension: pH 4–7L, 18 cm in length; 2nd dimension: 12% polyacrylamide. Arrows and numbers indicate the differentially expressed spots identified by LC/MS/MS. In red: proteins correlated with microarray data. In blue: proteins not correlated with microarray data.

The involvement of chemokine Cxcl2 (or Mip-2) in inflammation associated to vascular injury has been poorly investigated. Only recently Jabs A *et al.* demonstrated, in agreement with our data, its early activation after angioplasty [20]. Further studies will be necessary to clarify the role of Mip-2 in restenosis.

The collagen matrix constitutes a major portion of the vascular ECM and imparts blood vessels with tensile strength and, even more important, modulates SMC responses via specific receptors and signalling pathways. Cell migration, proliferation and general tissue remodelling related to vascular injury is enabled by degradation of the matrix scaffold by Matrix Metalloproteinases (MMPs). The equilibrium between ECM protein synthesis and MMP activity results to be impaired during restenosis. We detected a slight decrease of collagen type I α 2 (Col1a2) as well as of Col3a1, 48 hrs after arteriotomy, while Col1a1 showed a temporary decrease 48 hrs after injury, followed by an increase 7 days after arteriotomy. Conversely, microarray data included a marked and sustained increase of mRNAs coding for other collagen types, including Col12a1, Col5a1, Col11a1, Col9a3 and Col14a1. It has

been hypothesized that the adventitial and medial collagen deposition occurring early after vascular injury does not have an immediate effect on lumen narrowing, but it possibly stabilizes the vessel wall and impairs compensatory outward remodelling [21]. At later stages, collagen accumulation leads to constrictive remodelling after vascular injury [22].

The metabolism of collagens and of other ECM proteins is strongly linked to inflammation. In particular, ECM protein synthesis is highly regulated by different cytokines at the transcriptional level. Especially, TGF-β1, a key player in the pathophysiology of tissue repair, enhances type I collagen gene expression. In contrast, tumour necrosis factor α (TNF- α), whose matrix-remodelling function is opposite to that of TGF-β1, reduces type I collagen gene expression [23]. Our microarray data included members of both signalling pathways triggered by these cytokines (*e.g.* mothers against decapentaplegic homologs (SMAD)).

The collagen prolyl 4-hydroxylases (P4Hs), enzymes residing within the endoplasmic reticulum, have a central role in the biosynthesis of collagens [24]. Microarray data included a significant

Table 3 Differentially expressed protein spots in arteriotomy-injured WKY rat carotids. Data are expressed as densitometric values of spots in analytical gels, and as injured/uninjured carotid ratio. Densitometric values reported for spots derive from a mean of 5 different carotids ± S.D. In bold are reported variations in comparison to uninjured carotids. §: spots 1036 and 6703; ^: spots 6820, 6958 and 6825 are part of charge trains representing different post-translational modifications (PTM) of the same proteins. *: $P<0.05$ versus uninjured carotids.

Spot	Protein identity	GO category (Biological process)	Uninjured carotid	4 hrs after injury	48 hrs after injury	7 days after injury	4 hrs/ Uninjured carotid	48 hrs/ Uninjured carotid	7 days/ Uninjured carotid	Gel resolved pI	Gel resolved MW (Da)	Theoretical pI	Theoretical MW (Da)	No. Peptides Matched	Sequence coverage	Mascot score
1706	Guanine nucleotide-binding protein	Signal transduction	0.118 ± 0.13	0.107 ± 0.05*	absent	absent	0.90*			5.43	33560	5.6	37307	4	20%	89
6703§ (Mixture)	Contrapsin-like protease inhibitor 6 precursor	Protein metabolism	0.13 ± 0.02	0.07 ± 0.07	**0.74 ± 0.4***	0.42 ± 0.05	0.54	5.7*	3.23	4.65	51570	5.33	46622	22	63%	104
	Vimentin	Cytoskeleton and contractile apparatus								4.65	51570	5.06	53569	11	39%	93
1036§ (Mixture)	Contrapsin-like protease inhibitor 6 precursor	Protein metabolism	0.13 ± 0.02	0.09 ± 0.08	**0.67 ± 0.4***	0.23 ± 0.09	0.69	5.15*	1.76	4.7	50960	5.33	46622	23	64%	116
	Lumican precursor	Extracellular matrix and adhesion								4.7	50960	6	38255	7	24%	61
6820^	Haptoglobin precursor	Protein metabolism/acute phase response	absent	absent	**0.40 ± 0.28**	**0.20 ± 0.14**				4.98	34410	6.1	38525	15	41%	71
6958^	Haptoglobin precursor	Protein metabolism/stress response	0.014 ± 0.004	0.02 ± 0.005	**0.78 ± 0.1***	0.16 ± 0.10	1.43	55.71*	11.4	5.47	33720	6.1	38525	16	47%	79
6825^	Haptoglobin precursor	Protein metabolism/stress phase response	0.04 ± 0.02	0.06 ± 0.04	**0.84 ± 0.29***	0.4 ± 0.21	1.5	21*	10	5.29	33790	6.1	38525	19	47%	82
1340 (Mixture)	Tubulin beta chain	Cytoskeleton and contractile apparatus	absent	absent	absent	**0.05 ± 0.02**				6.12	43490	4.78	49829	10	33%	56
	Adenosylhomocysteinase (EC 3.3.1.1)	Carbohydrate metabolism								6.12	43490	6.08	47376	11	41%	59
	TAR DNA-binding protein-43 (TDP-43)	Nucleic acid metabolism								6.12	43490	6.26	44519	5	23%	74
3759 (Mixture)	Actin, alpha skeletal muscle (alpha-actin 1)	Cytoskeleton and contractile apparatus	0.56 ± 0.39	0.87 ± 0.44	0.73 ± 0.28	**1.58 ± 0.47***	1.55	1.30	**2.82***	5.38	27720	5.23	42024	15	50%	176
	Heat-shock protein beta-1 (HspB1) (Heat shock 27 kDa protein) (HSP 27)	Stress response								5.38	27720	6.12	22879	5	38%	65

Table 3 Continued

Spot	Protein identity	GO category (Biological process)	Uninjured carotid	4 hrs after injury	48 hrs after injury	7 days after injury	4 hrs/ Uninjured carotid	48 hrs/ Uninjured carotid	7 days/ Uninjured carotid	Gel resolved pI	Gel resolved MW (Da)	Theoretical pI	Theoretical MW (Da)	No. Peptides Matched	Sequence coverage	Mascot score
6634	Heat shock cognate 71 kDa protein	Stress response	0.53 ± 0.28	0.45 ± 0.21	0.31 ± 0.15	**0.12 ± 0.06***	0.85	0.58	0.23*	5.31	65250	5.37	70827	34	63%	119
6812	Actin, alpha cardiac	Cytoskeleton and contractile apparatus	1.26 ± 0.57	0.7 ± 0.3	1.89 ± 0.56	**2.94 ± 0.48***	0.55	1.5	2.3*	5.42	35470	5.23	41992	22	69%	145
6881	Actin, aortic smooth muscle (Alpha-actin 2)	Cytoskeleton and contractile apparatus	0.52 ± 0.34	0.22 ± 0.23	0.76 ± 0.09	**1.48 ± 0.43***	0.42	1.46	2.85*	5.43	29310	5.23	41982	13	39%	155
1690	Tropomyosin beta chain (Tropomyosin 2)	Cytoskeleton and contractile apparatus				**0.12 ± 0.07**				4.65	32630	4.66	32817	14	44%	93
1595	Malate dehydrogenase 1, NAD (soluble)	Carbohydrate metabolism			**0.08 ± 0.06**	**0.05 ± 0.04**				6.01	35090	5.93	36461	8	44%	92
1719 (Mixture)	Mimecan precursor (Osteoglycin)	N.D.		**0.169 ± 0.1**						5.6	32570	5.52	33991	7	25%	113
	F-actin capping protein alpha-2 subunit (CapZ alpha-2)	Cytoskeleton and contractile apparatus								5.6	32570	5.58	32816	5	24%	57
7104	F-actin capping protein beta subunit (CapZ beta)	Cytoskeleton and contractile apparatus		**0.176 ± 0.08**	**0.044 ± 0.02**					5.48	30570	5.47	31195	13	53%	98
5126	Gelsolin	Cytoskeleton and contractile apparatus	0.022 ± 0.01	**0.019 ± 0.01***			**0.86***			5.5	84490	5.76	86014	2	25%	76

3-fold increase of prolyl 4-hydroxylase, β polypeptide 48 hrs after arteriotomy (P<0.001). Interacting Spp1 (also known as osteopontin) and CD44 (a cell surface receptor for hyaluronan), both increased in arteriotomy-injured carotids, as well as in angioplasty-injured carotids [10] may also play a major role in ECM modulation and consequently in vascular remodelling.

For what concerns the MMP differential expression, we detected a significant (P<0.0001), massive up-regulation of MMPs 9, 12, 13 and 15, ranging from 4 hrs to 7 days after arteriotomy. Conversely, we found a slight increase only of TIMP1 4 hrs and 48 hrs after injury.

Most genes for MMPs are inducible if the tissue, whether under physiological or pathological conditions, is remodelled. The increase of MMP9, MMP12 and MMP13 could be at least in part induced by the increased expression of pro-inflammatory cytokines included among microarray data, for example IL-1 β [25–27]. These data further support a spatial reorganization of structural elements after arteriotomy that leads to a constrictive remodelling.

TIMP1 increased expression we observed can be modulated by cytokines (e.g. TNF-α) trough the induction of nuclear transcription factors. Interestingly, TIMP1 has been demonstrated to be able to form a specific complex with pro-MMP9, whose mRNA is markedly up-regulated after arteriotomy, thus suggesting a coordinate activation of both molecules after vascular injury.

Our overall data concerning the expression profiles of collagen types are in agreement with results of Li JM *et al.* [10], except that for Col14a1, Col9a3 and Col11a1, that are not included among microarray results obtained in angioplasty-injured carotids. Conversely, the microarray data sets obtained in the two models of vascular injury did not share common features concerning the MMP and TIMP family members, as the microarray data obtained by Li JM *et al.* [10] in the model of rat carotid angioplasty included only a slight increase of MMP14, and a slight decrease of TIMP2, further

Table 4 Correlation between proteomics and microarray data. Proteomics data are expressed as densitometric values of spots in analytical gels and as ratio between injured/uninjured carotid values. Microarray data are expressed as fold-change (FC) of variation in comparison to carotids from uninjured rats. In bold are reported significant protein variations in comparison to uninjured carotids. §: spots 1036 and 6703; ^: spots 6820, 6958 and 6825 are part of charge trains representing different PTM of the same proteins. *: $P<0.05$ versus uninjured carotids; **: $P<0.0001$ *versus* uninjured carotids.

Protein identity	GO category (Biological process)	Protein Spot	Proteomics data							Microarray data			
			Uninjured carotid	4 hrs after injury	48 hrs after injury	7 days after injury	4 hrs/ Uninjured carotids	48 hrs/ Uninjured carotids	7 days/ Uninjured carotids	Affymetrix Probe Set ID	4 hrs/ Uninjured carotids	48 hrs/ Uninjured carotids	7 days/ Uninjured carotids
Guanine nucleotide-binding protein	Signal transduction	1706	0.118 ± 0.13	**0.107 ± 0.05***			0.90*			1370867_at	0.363**		
Contrapsin-like protease inhibitor 6 precursor	Protein metabolism	6703§	0.13 ± 0.02	0.07 ± 0.07	**0.74 ± 0.4***	0.42 ± 0.05	0.54	5.7*	3.23	1368224_at	32.91**	73.46**	3.93**
Contrapsin-like protease inhibitor 6 precursor	Protein metabolism	1036§	0.13 ± 0.02	0.09 ± 0.08	**0.67 ± 0.4***	0.23 ± 0.09	0.69	5.15*	1.76	1368224_at	32.91**	73.46**	3.93**
Haptoglobin precursor	Protein metabolism/stress response	6820^			**0.40 ± 0.28**	**0.20 ± 0.14**				1370148_at	21.86**	3.83**	
Haptoglobin precursor	Protein metabolism/stress response	6958^	0.014 ± 0.004	0.02 ± 0.005	**0.78 ± 0.1***	0.16 ± 0.10	1.43	**55.71***	11.4	1370148_at	21.86**	3.83**	
Haptoglobin precursor	Protein metabolism/stress response	6825^	0.04 ± 0.02	0.06 ± 0.04	**0.84 ± 0.29***	0.4 ± 0.21	1.5	21*	10	1370148_at	21.86**	3.83**	
Tubulin beta chain	Cytoskeleton and contractile apparatus	1340 (mixture)				**0.05 ± 0.02**				1388131_at	5.89**	2.57**	7.62**
Adenosylhomocysteinase (EC 3.3.1.1)	Carbohydrate metabolism	1340 (mixture)				**0.05 ± 0.02**				1367798_at	2.96**		
TAR DNA-binding protein-43 (TDP-43)	Nucleic acid metabolism	1340 (mixture)				**0.05 ± 0.02**				1371367_at	3.85**	2.97**	
Actin, alpha skeletal muscle (alpha-actin 1)	Cytoskeleton and contractile apparatus	3759	0.56 ± 0.39	0.87 ± 0.44	0.73 ± 0.28	**1.58 ± 0.47***	1.55	1.30	**2.82***	1369928_at	5.688**		24.12**
Actin, alpha cardiac	Cytoskeleton and contractile apparatus	6812	1.26 ± 0.57	0.7 ± 0.3	1.89 ± 0.56	**2.94 ± 0.48***	0.55	1.5	2.3*	1370856_at			6.218**

supporting the role played by negative remodelling in the arteriotomy model of stenosis.

Finally, our microarray data included also an increase of different cathepsins. Cathepsin cysteine proteases have a central role in ECM remodelling and have been implicated in the development and progression of cardiovascular diseases. In particular, microarray data revealed a marked and sustained increase of mRNAs coding for cathepsins S, B and Z after carotid arteriotomy. Cathepsin S has already been demonstrated to digest laminin, fibronectin and type I collagen and be associated to invading SMCs, macrophages and foam cells [28], thus highlighting its importance in the pathogenesis of vascular stenosis. A similar increase of cathepsins S and Z, but not of cathepsin B, has been highlighted also in angioplasty-injured rat carotids [10]. The role of cathepsins B and Z in arterial stenosis remains to be further elucidated.
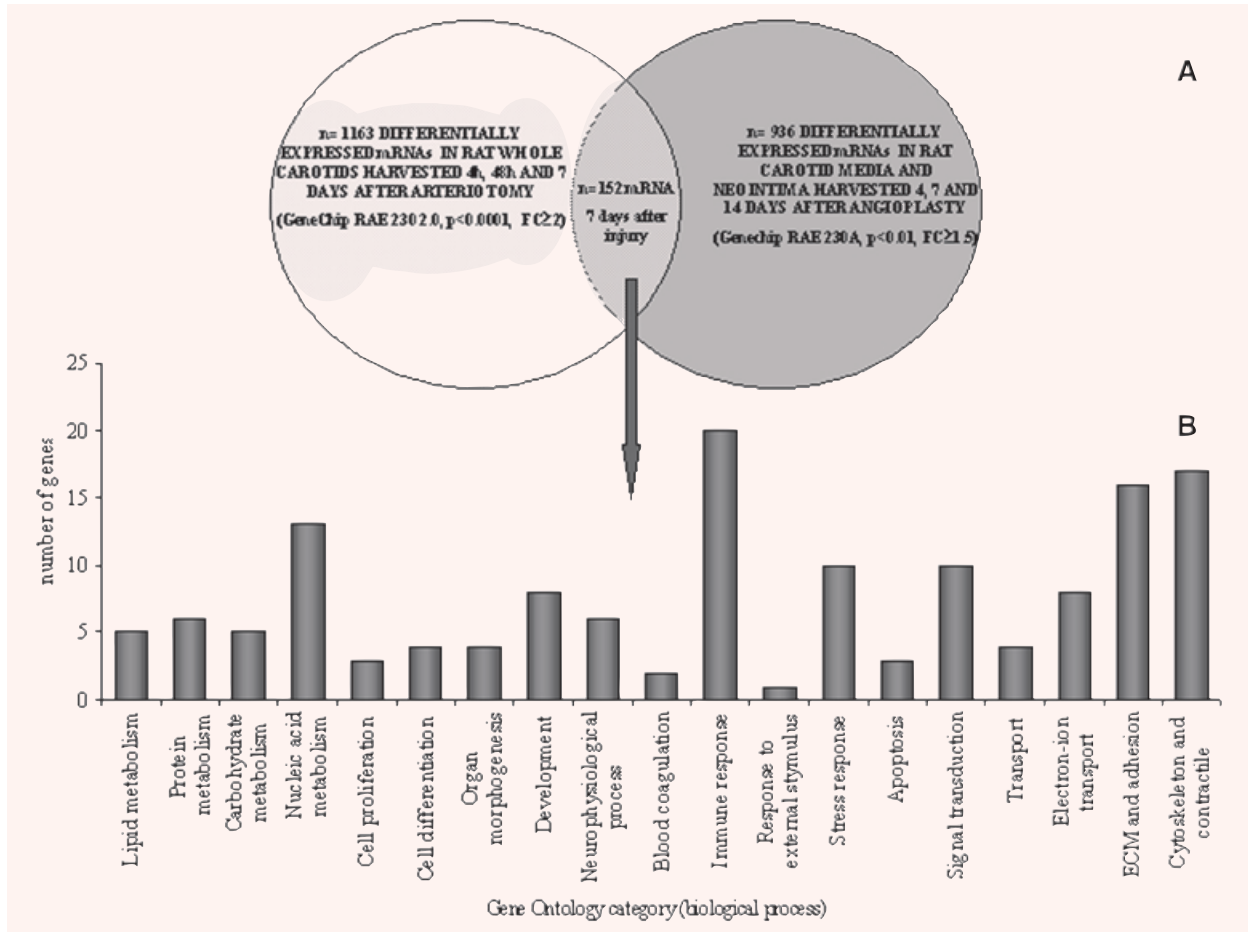
Fig. 6 (**A**) Venn diagram resulting from a direct comparison between microarray data obtained in arteriotomy- and in angioplasty-injured carotids harvested 7 days after procedure [10]; (**B**) GO functional classification of genes modulated both by arteriotomy and angioplasty in rat carotids 7 days after the procedure.

Myofibroblasts, already known to exacerbate vessel remodelling and to contribute to neointima formation after vascular injury [29], could play a major role in arteriotomy, since the denuded surface area of wounded tissue is greater than in angioplasty and involves the adventitia, where fibroblasts differentiate to myofibroblasts. The concurrent events known to be necessary to trigger the formation of these cells (mechanical stress, activation of TGF-β1 pathway and expression of the ED-A Fn isoform) [30] are present in our model of arteriotomy. Myofibroblasts are important actors in stenosis progression also because they can modulate the inflammatory response and be responsive to IL-6 [31]. The sustained activation of the focal adhesion pathway after arteriotomy (Table 1), together with regulation of actin cytoskeleton pathway (Sup. File 6), may play a role not only in migration and proliferation of SMCs, but also in myofibroblast differentiation, force generation and transmission. Therapies targeting myofibroblast differentiation or contraction would be of great interest for limitation of surgically-induced (re)stenosis. Some approaches have already been tested in this concern [32], but they have not yet been applied in models of vascular injury.

ROS formation and elimination, under physiological conditions, are well balanced. Enhanced activity of oxidant enzymes and/or reduced activity of antioxidant enzymes, lead to the pathologic state of oxidative stress. Microarray data indicated the activation of a number of molecules involved in ROS production (the NAD(P)H oxidase subunits 22phox, gp91phox and Ncf4, the small GTPase Rac2). The contemporary increase of the antioxidant Sod2 is presumably due to compensatory mechanisms. We hypothesize that ROS production is increased also by short-term systemic alterations of haemodynamic forces (occurring during and after arteriotomy), then mechanotransduced in vascular cells. Nevertheless, it should be underlined that our hypotheses about the roles played by ROS production after arteriotomy are speculative, since did not measured experimentally the actual production of ROS.
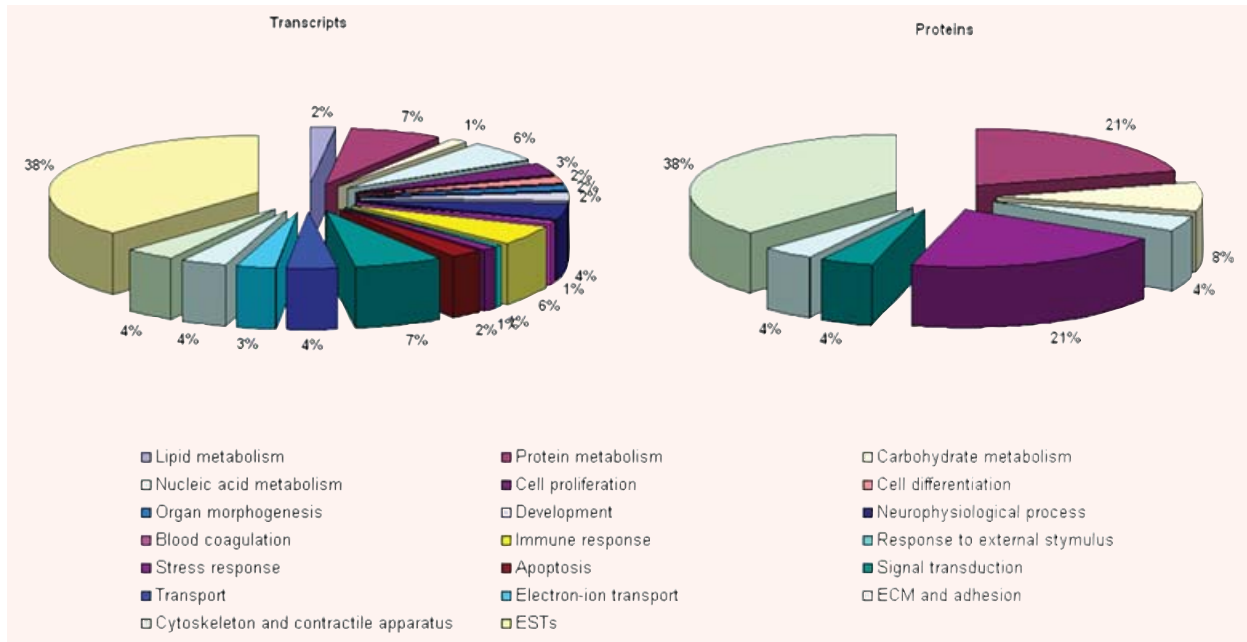
Fig. 7 Pie charts of GO functional categories including genes differentially expressed at any point (4 hrs, 48 hrs or 7 days) in arteriotomy-injured rat carotids at transcript or protein level. Data are based on the 1163 differentially expressed mRNAs identified by microarrays and on the 19 differentially expressed proteins identified by 2D-gel and LC/MS/MS.

Catecholamines have vasoconstrictive and growth factor-like activities. Our data indicate variations of perivascular innervations of arteriotomy-injured carotids that could have relevance on vessel contractility/relaxation. Studies highlighted the degeneration followed by reinnervation of arterial grafts by adrenergic nerves [33] and the increase of adrenergic neurotransmission after angioplasty [34], suggesting that the rapid liberation of catecholamines from degenerating adrenergic nerves may have an important role in early vasospasm in vascular surgery. Our data on markers of axonal growth are partially different from others [33] since we detected an increase of neurofilaments and of growth-associated protein 43, together with a marked increase of Dbh, but also an apparently contrasting decrease of transmitter-synthesizing enzyme mRNAs (neuronal NOS and tyrosine hydroxylase) (P<0.001). The increase of perivascular cholinergic receptors Chrna7 and Chrnd has been detected for the first time in a model of vascular injury.

Among transcription factors involved in switching of SMC phenotype in response to environmental cues, KLF family of zinc finger factors has recently received increased attention. Many of the 16 known KLF members show developmental and pathological implications in the vasculature [35]. Our data confirm the increase of KLF4, KLF5 and KFL6 expression after vascular injury, revealed by other studies [36, 37]. Of interest, our data highlight for the first time the involvement of KFL10 and KLF15 in progression of surgically-induced vascular injury. While KLF4-6 are known to act as activators of transcription, KLF10 and KLF15 are mainly repres-

sors of transcriptional activity, and showed an opposite behaviour after arteriotomy, as KLF10 was increased while KLF15 showed a persistent decrease after arteriotomy. Further studies will be necessary to clarify their role in SMC phenotype switching after vascular injury.

Proteomic data confirmed and extended microarray results

Proteomic analysis led to the identification of 19 differentially expressed proteins that validated and extended the microarray data, revealing also time-dependent PTM for Hsp27, haptoglobin and Serpina3n (Table 3, 4).

Haptoglobin is a tetrameric acute phase glycoprotein produced mainly in the liver but also in other tissues, including the arterial wall [38]. Our results are in agreement with studies [39] highlighting the activation after angioplasty of an arterial haptoglobin characterized by a unique set of glycoforms whose functional role remains to be elucidated.

Serpina3n is mainly of hepatic origin, but it has been identified also in other cell types, including ECs [40]. We cannot exclude that Serpina3n protein identified in carotids derives from serum infiltration, and not from a synthesis *in situ*. Nevertheless, the arteriotomy-induced 76-fold increase of the Serpina3n mRNA makes reasonable to argue a subsequent increase also of the protein. In

case, this would be the first demonstration of the involvement of Serpina3n in (re)stenosis, presumably with a role in preventing degenerative proteolysis induced by inflammatory cells and in cell spreading by inhibiting the degradation of Fn [41]. The role of the different glycoforms of Serpina3n we identified should also be elucidated.

Overall proteomic data support a contractile reaction of carotids since 7 days arteriotomy, indicated by the decrease of the actin depolymerization factor gelsolin and of F-actin capping protein β subunit (required for barbed end actin filament capping activity) [42]. Hsp27 regulates the actin filament dynamics and undergoes phosphorylation under stress conditions, binding tropomyosin (increased 7 days after arteriotomy) and facilitating SMC contraction [43]. In agreement with these studies, the Hsp27 isoform that increased 7 days after arteriotomy showed a gel resolved pI of 5.38, compatible with the pI of 5.44 (calculated by Expasy's Compute pI/Mw program), corresponding to the presence of three phosphate groups at the known phosphorylation sites Ser_{13}, Ser_{15} and Ser_{86}. It is of interest that while microarray analysis did not reveal changes of Hsp27 mRNA, proteomic analysis allowed the detection of PTM of this protein occurring after arteriotomy.

Conclusions

This is the first study that conjugates two high-throughput methods to assess gene expression changes in a model of (re)stenosis, showing the complementary potentialities of this combined investigation, since we found a correlation only for 47% of proteins with the corresponding mRNAs, due to the different sensitivity of the techniques, to molecule stability and to different mechanisms of regulation.

The gene lists generated in this study include novel potential targets for restenosis prevention. Antiproliferative approaches showed promising results in animals but were often ineffective in humans. Considering that inflammation/oxidative stress, signal transduction, focal adhesion and remodelling proved to be markedly activated by arteriotomy, we suggest to shift experimental therapies towards a multi-factorial antagonism of these processes and to a selective inhibition of myofibroblasts, supposed to play a major role in exacerbating wound healing triggered by vascular surgical injury.

Acknowledgements

References

1. **Morice MC, Serruys PW, Sousa JE, Fajadet J, Ban Hayashi E, Perin M, Colombo A, Schuler G, Barragan P, Guagliumi G, Molnar F, Falotico R.** A randomized comparison of a sirolimus-eluting stent with a standard stent for coronary revascularization. *N Engl J Med.* 2002; 346: 1773–80.

2. **Camenzind E.** Treatment of in-stent restenosis–back to the future? *N Engl J Med.* 2006; 355: 2149–51.

3. **Legrand V.** Therapy insight: diabetes and drug-eluting stents. *Nat Clin Pract Cardiovasc Med.* 2007; 4: 143–50.

4. **Kastrup A, Groschel K.** Carotid endarterectomy *versus* carotid stenting: an updated review of randomized trials and subgroup analyses. *Acta Chir Belg.* 2007; 107: 119–28.

5. **Forte A, Esposito S, De Feo M, Galderisi U, Quarto C, Esposito F, Renzulli A, Berrino L, Cipollaro M, Agozzino L, Cotrufo M, Rossi F, Cascino A.** Stenosis progression after surgical injury in Milan hypertensive rat carotid arteries. *Cardiovasc Res.* 2003; 60: 654–63.

6. **Forte A, Galderisi U, De Feo M, Gomez MF, Esposito S, Sante P, Renzulli A, Agozzino L, Hellstrand P, Berrino L, Cipollaro M, Cotrufo M, Rossi F, Cascino A.** c-Myc antisense oligonucleotides preserve smooth muscle differentiation and reduce negative remodelling following rat carotid arteriotomy. *J Vasc Res.* 2005; 42: 214–25.

7. **Mijalski T, Harder A, Halder T, Kersten M, Horsch M, Strom TM, Liebscher HV, Lottspeich F, de Angelis MH, Beckers J.** Identification of coexpressed gene clusters in a comparative analysis of transcriptome and proteome in mouse tissues. *Proc Natl Acad Sci USA.* 2005; 102: 8621–6.

8. **Eberwine J.** Amplification of mRNA populations using aRNA generated from immobilized oligo(dT)-T7 primed cDNA. *Biotechniques.* 1996; 20: 584–91.

9. **Patel OV, Suchyta SP, Sipkovsky SS, Yao J, Ireland JJ, Coussens PM, Smith GW.** Validation and application of a high fidelity mRNA linear amplification procedure for profiling gene expression. *Vet Immunol Immunopathol.* 2005; 105: 331–42.

10. **Li JM, Zhang X, Nelson PR, Odgren PR, Nelson JD, Vasiliu C, Park J, Morris M, Lian J, Cutler BS, Newburger PE.** Temporal evolution of gene expression in rat carotid artery following balloon angioplasty. *J Cell Biochem.* 2007; 101: 399–410.

11. **Aavik E, Mahapatra A, Boldrick J, Chen X, Barry C, Dutoit D, Sarwal M, Hayry P.** Correlation between gene expression and morphological alterations in baboon carotid after balloon dilatation injury. *Faseb J.* 2005; 19: 130–2.

12. **Mayr M, Mayr U, Chung YL, Yin X, Griffiths JR, Xu Q.** Vascular proteomics: linking proteomic and metabolomic changes. *Proteomics.* 2004; 4: 3751–61.

13. **Mayr U, Mayr M, Yin X, Begum S, Tarelli E, Wait R, Xu Q.** Proteomic dataset of mouse aortic smooth muscle cells. *Proteomics.* 2005; 5: 4546–57.

14. **Dupont A, Corseaux D, Dekeyzer O, Drobecq H, Guihot AL, Susen S, Vincentelli A, Amouyel P, Jude B, Pinet F.** The proteome and secretome of human arterial smooth muscle cells. *Proteomics.* 2005; 5: 585–96.

15. **Bruneel A, Labas V, Mailloux A, Sharma S, Vinh J, Vaubourdolle M, Baudin B.** Proteomic study of human umbilical vein endothelial cells in culture. *Proteomics.* 2003; 3: 714–23.

16. **Hojo Y, Ikeda U, Katsuki T, Mizuno O, Fukazawa H, Kurosaki K, Fujikawa H, Shimada K.** Release of endothelin 1 and angiotensin II induced by percutaneous transluminal coronary angioplasty. *Catheter Cardiovasc Interv.* 2000; 51: 42–9.

17. **Brasier AR, Recinos A, 3rd, Eledrisi MS.** Vascular inflammation and the renin-angiotensin system. *Arterioscler Thromb Vasc Biol.* 2002; 22: 1257–66.

18. **Inami N, Nomura S, Shimazu T, Manabe K, Kimura Y, Iwasaka T.** Adiponectin incompletely prevent MCP-1-dependent restenosis after percutaneous coronary intervention in patients with coronary artery disease. *J Thromb Thrombolysis.* 2007; 24: 267–73.

19. **Wei LH, Jacobs AT, Morris SM, Jr., Ignarro LJ.** IL-4 and IL-13 upregulate arginase I expression by cAMP and JAK/STAT6 pathways in vascular smooth muscle cells. *Am J Physiol Cell Physiol.* 2000; 279: C248–56.

20. **Jabs A, Okamoto E, Vinten-Johansen J, Bauriedel G, Wilcox JN.** Sequential patterns of chemokine- and chemokine receptor-synthesis following vessel wall injury in porcine coronary arteries. *Atherosclerosis.* 2007; 192: 75–84.

21. **Schmidt MR, Maeng M, Kristiansen SB, Andersen HR, Falk E.** The natural history of collagen and alpha-actin expression after coronary angioplasty. *Cardiovasc Pathol.* 2002; 13: 260–7.

22. **Lafont A, Durand E, Samuel JL, Besse B, Addad F, Levy BI, Desnos M, Guerot C, Boulanger CM.** Endothelial dysfunction and collagen accumulation: two independent factors for restenosis and constrictive remodeling after experimental angioplasty. *Circulation.* 1999; 100: 1109–15.

23. **Verrecchia F, Mauviel A.** TGF-beta and TNF-alpha: antagonistic cytokines controlling type I collagen gene expression. *Cell Signal.* 2004; 16: 873–80.

24. **Myllyharju J.** Prolyl 4-hydroxylases, the key enzymes of collagen biosynthesis. *Matrix Biol.* 2003; 22: 15–24.

25. **Burrage PS, Huntington JT, Sporn MB, Brinckerhoff CE.** Regulation of matrix metalloproteinase gene expression by a retinoid X receptor-specific ligand. *Arthritis Rheum.* 2007; 56: 892–904.

26. **Liang KC, Lee CW, Lin WN, Lin CC, Wu CB, Luo SF, Yang CM.** Interleukin-1beta induces MMP-9 expression via p42/p44 MAPK, p38 MAPK, JNK, and nuclear factor-kappaB signaling pathways in human tracheal smooth muscle cells. *J Cell Physiol.* 2007; 211: 759–70.

27. **Xie S, Issa R, Sukkar MB, Oltmanns U, Bhavsar PK, Papi A, Caramori G, Adcock I, Chung KF.** Induction and regulation of matrix metalloproteinase-12 in human airway smooth muscle cells. *Respir Res.* 2005; 6: 148.

28. **Burns-Kurtis CL, Olzinski AR, Needle S, Fox JH, Capper EA, Kelly FM, McQueney MS, Romanic AM.** Cathepsin S expression is up-regulated following balloon angioplasty in the hypercholesterolemic rabbit. *Cardiovasc Res.* 2004; 62: 610–20.

29. **Shi Y, O'Brien JE, Fard A, Mannion JD, Wang D, Zalewski A.** Adventitial myofibroblasts contribute to neointimal formation in injured porcine coronary arteries. *Circulation.* 1996; 94: 1655–64.

30. **Hinz B.** Formation and function of the myofibroblast during tissue repair. *J Invest Dermatol.* 2007; 127: 526–37.

31. **Okamoto E, Couse T, De Leon H, Vinten-Johansen J, Goodman RB, Scott NA, Wilcox JN.** Perivascular inflammation after balloon angioplasty of porcine coronary arteries. *Circulation.* 2001; 104: 2228–35.

32. **Hinz B, Gabbiani G, Chaponnier C.** The NH2-terminal peptide of alpha-smooth muscle actin inhibits force generation by the myofibroblast *in vitro* and *in vivo. J Cell Biol.* 2001; 157: 657–63.

33. **Heikki P, Timo W, Nureddin A, Sampsa V.** Degeneration and regeneration of perivascular innervation in arterial grafts. *J Craniofac Surg.* 2004; 15: 570–81.

34. **Candipan RC, Hsiun PT, Pratt R, Cooke JP.** Vascular injury augments adrenergic neurotransmission. *Circulation.* 1994; 89: 777–84.

35. **Suzuki T, Aizawa K, Matsumura T, Nagai R.** Vascular implications of the Kruppel-like family of transcription factors. *Arterioscler Thromb Vasc Biol.* 2005; 25: 1135–41.

36. **Sakamoto H, Sakamaki T, Kanda T, Hoshino Y, Sawada Y, Sato M, Sato H, Oyama Y, Nakano A, Takase S, Hasegawa A, Nagai R, Kurabayashi M.** Smooth muscle cell outgrowth from coronary atherectomy specimens *in vitro* is associated with less time to restenosis and expression of a key Transcription factor KLF5/BTEB2. *Cardiology.* 2003; 100: 80–5.

37. **Liu Y, Sinha S, McDonald OG, Shang Y, Hoofnagle MH, Owens GK.** Kruppel-like factor 4 abrogates myocardin-induced activation of smooth muscle gene expression. *J Biol Chem.* 2005; 280: 9719–27.

38. **de Kleijn DP, Smeets MB, Kemmeren PP, Lim SK, Van Middelaar BJ, Velema E, Schoneveld A, Pasterkamp G, Borst C.** Acute-phase protein haptoglobin is a cell migration factor involved in arterial restructuring. *Faseb J.* 2002; 16: 1123–5.

39. **Smeets MB, Sluijter JP, Donners MM, Velema E, Heeneman S, Pasterkamp G, de Kleijn DP.** Increased arterial expression of a glycosylated haptoglobin isoform after balloon dilation. *Cardiovasc Res.* 2003; 58: 689–95.

40. **Forsyth KD, Talbot V, Beckman I.** Endothelial serpins–protectors of the vasculature? *Clin Exp Immunol.* 1994; 95: 277–82.

41. **Ikari Y, Fujikawa K, Yee KO, Schwartz SM.** Alpha(1)-proteinase inhibitor, alpha(1)-antichymotrypsin, or alpha(2)-macroglobulin is required for vascular smooth muscle cell spreading in three-dimensional fibrin gel. *J Biol Chem.* 2000; 275: 12799–805.

42. **McGregor E, Kempster L, Wait R, Gosling M, Dunn MJ, Powell JT.** F-actin capping (CapZ) and other contractile saphenous vein smooth muscle proteins are altered by hemodynamic stress: a proteonomic approach. *Mol Cell Proteomics.* 2004; 3: 115–24.

43. **Bitar KN.** HSP27 phosphorylation and interaction with actin-myosin in smooth muscle contraction. *Am J Physiol Gastrointest Liver Physiol.* 2002; 282: G894–903.